

# Selecting additional test locations to enhance the 24-2 pattern using a scoring system



Matthias Monhart<sup>1</sup>, Gary Lee<sup>2</sup>, Aiko Iwase<sup>3</sup>, John Flanagan<sup>4</sup>

<sup>1</sup> Carl Zeiss AG, Feldbach, Switzerland, <sup>2</sup> Carl Zeiss Meditec, Dublin CA, United States, <sup>3</sup> Tajimi Iwase Eye Clinic, Tajimi, Japan,

<sup>4</sup> University of California Berkeley, Berkeley, United States

WGCSUB-1642 / P-WT-309

## Purpose:

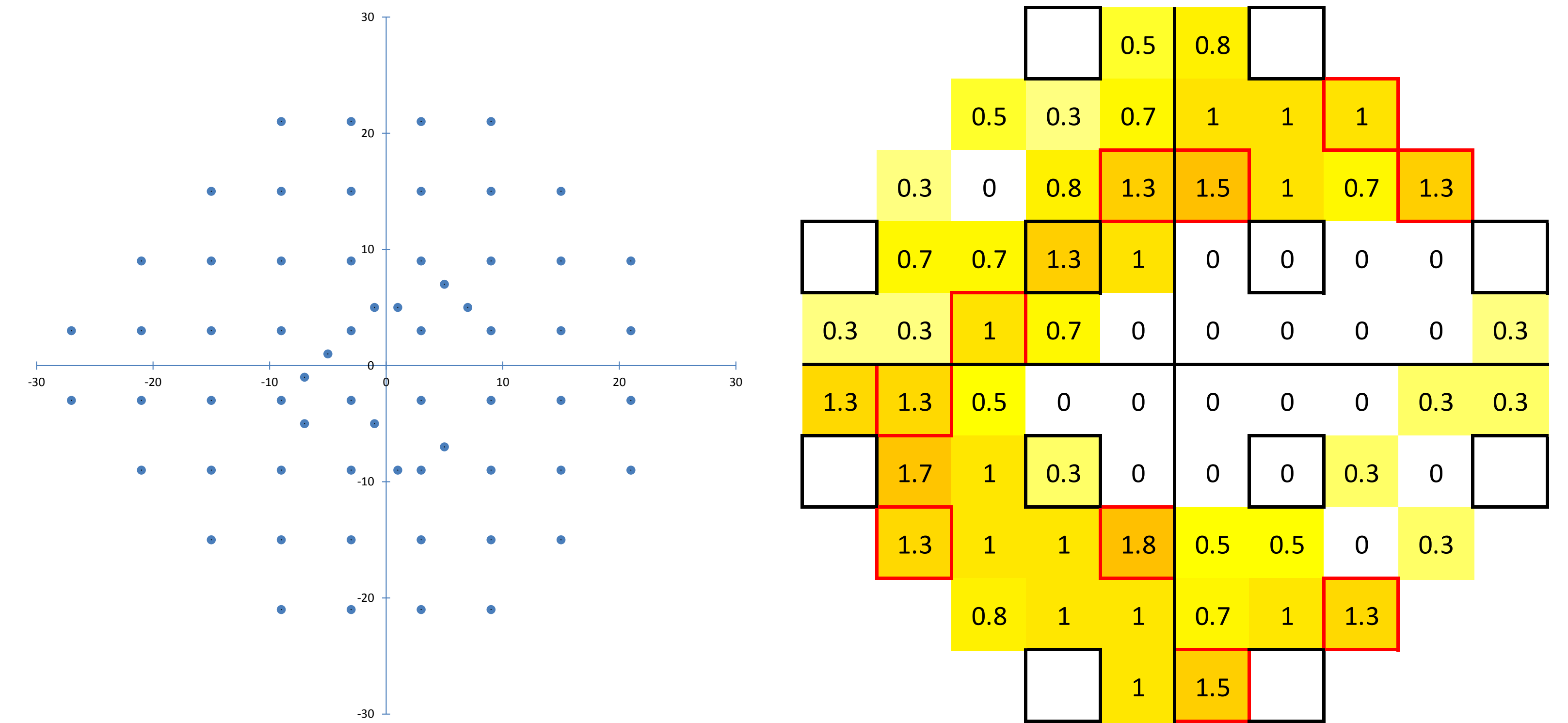
The 24-2 test pattern may underestimate and sometimes miss paracentral glaucomatous defects<sup>1,2</sup>. The goal of this study was to use past experience to select test locations from the 10-2 pattern to add to the 24-2 pattern so as to improve its capability for glaucoma detection and follow up. In order to minimize fatigue, only 10 additional test locations were added.

## Methods:

A small expert group in visual field testing and structure-function correlation was asked to suggest test locations from the 10-2 test pattern that may be added to the 24-2 pattern to improve the detection and follow up of paracentral glaucomatous defects<sup>3</sup>. Next, publications on the prevalence and depth of glaucomatous macular defects<sup>4,5,6,7,8</sup> were systematically evaluated and their regional information was entered into an Excel sheet. The superior field and the inferior field were evaluated separately. For each study, cut off values were defined to translate the study outcome into a number 0 ( $\leq 50$ th %ile), 1 ( $> 50$ th %ile) or 2 ( $> 90$ th %ile). The final score as in Figure 1b was then calculated as the average of all individual scores. Suggested test locations with a score of 1 or less were replaced with test locations with higher scores, applying the following rules: I) at least 2 new test locations per quadrant; II) selecting the highest scores. In a final step, a sanity check was performed with two previously not included studies: A study on visual field progression criteria<sup>9</sup> confirmed that the new and existing macular test locations cover 3 clusters with 3 or more test locations. A publication analyzing the vulnerability of the macula for glaucomatous damage using Optical Coherence Tomography<sup>10</sup> confirmed that the 2 most vulnerable zones are covered with 7 and 8 test locations respectively.

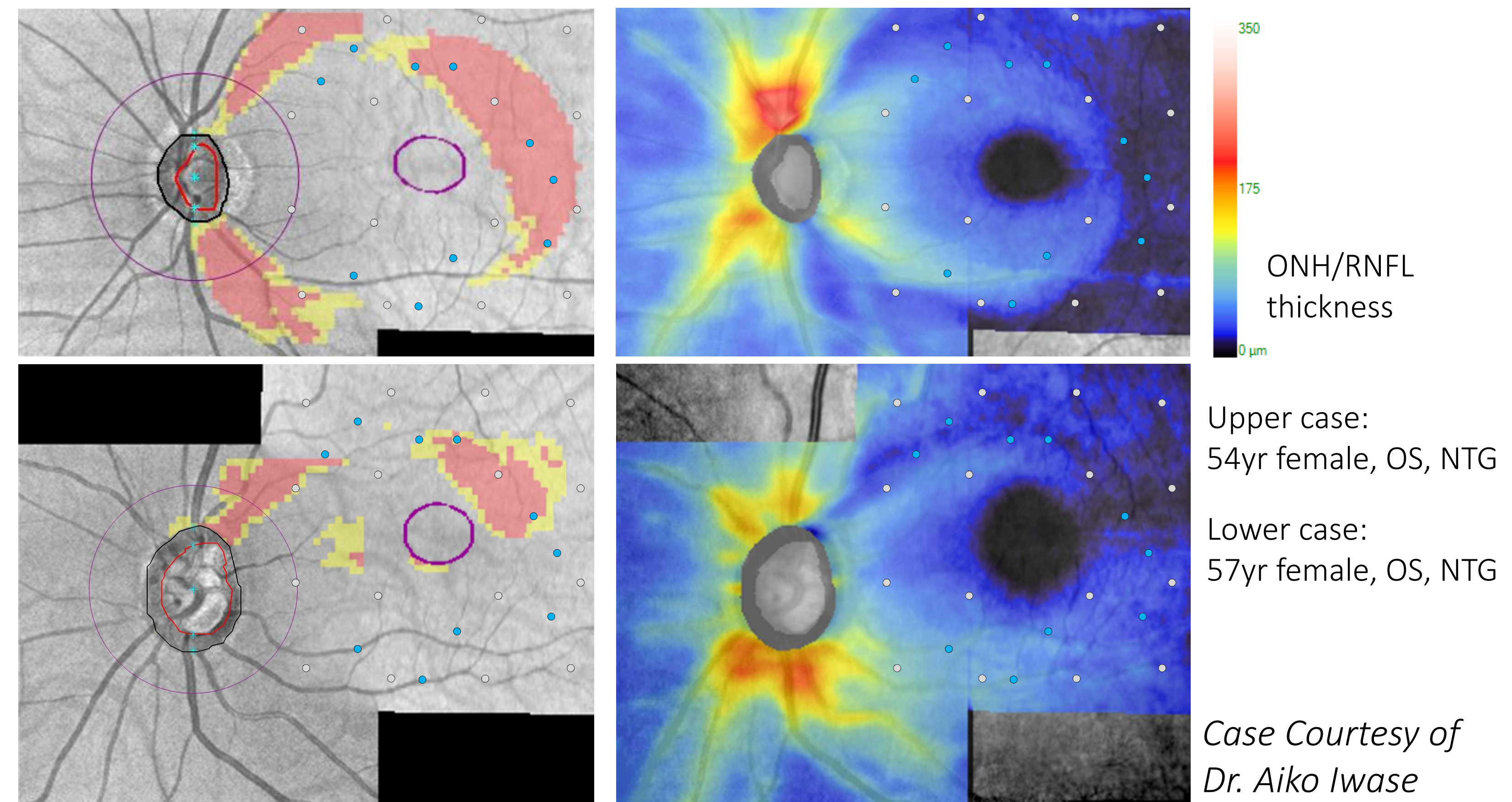
## Results:

The figure to the left shows the combined test pattern consisting of 64 test locations in OD orientation: All test locations from the 24-2 test pattern and 10 selected test locations from the 10-2 test pattern. The figure to the right shows the average scores for all 10-2 test locations on the 0-2 scale described under Methods and based on literature. The selected new test locations are marked with a red frame.



## Conclusions:

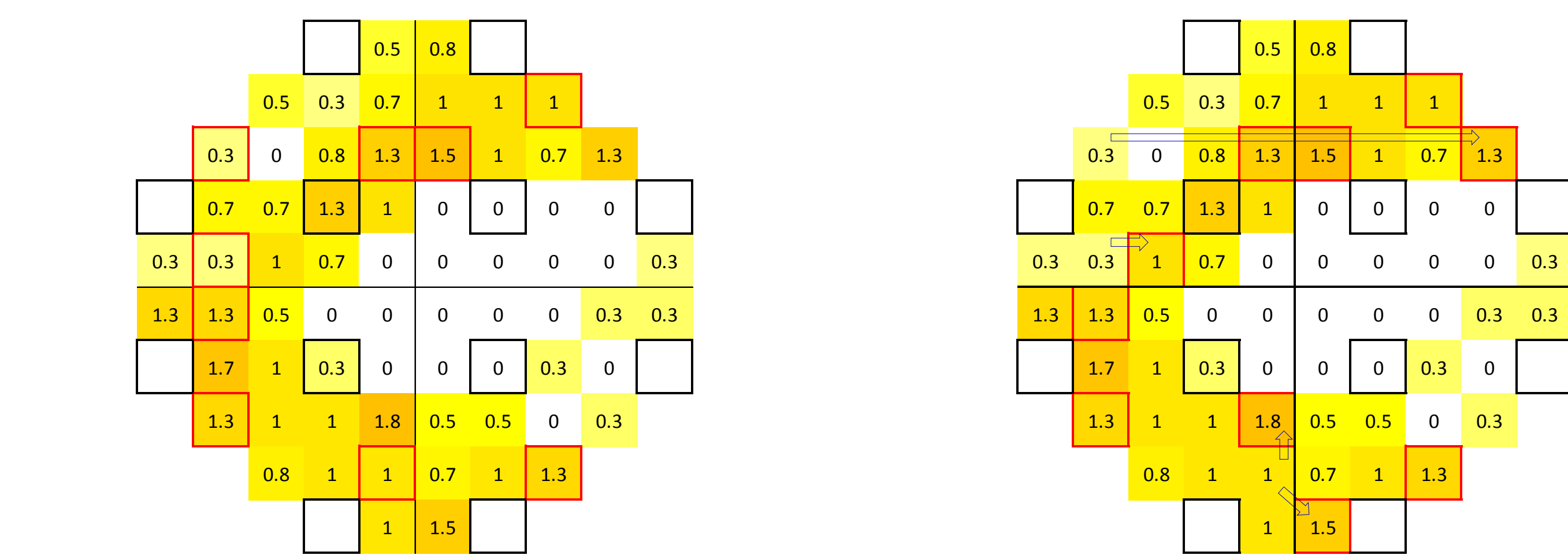
A new combined test pattern was created using the 24-2 test pattern as a basis and 10 test locations from the 10-2 test pattern. The selected test locations allow to form additional progression clusters in the macular area and cover areas known to be susceptible to glaucomatous defects both from structural and functional studies.



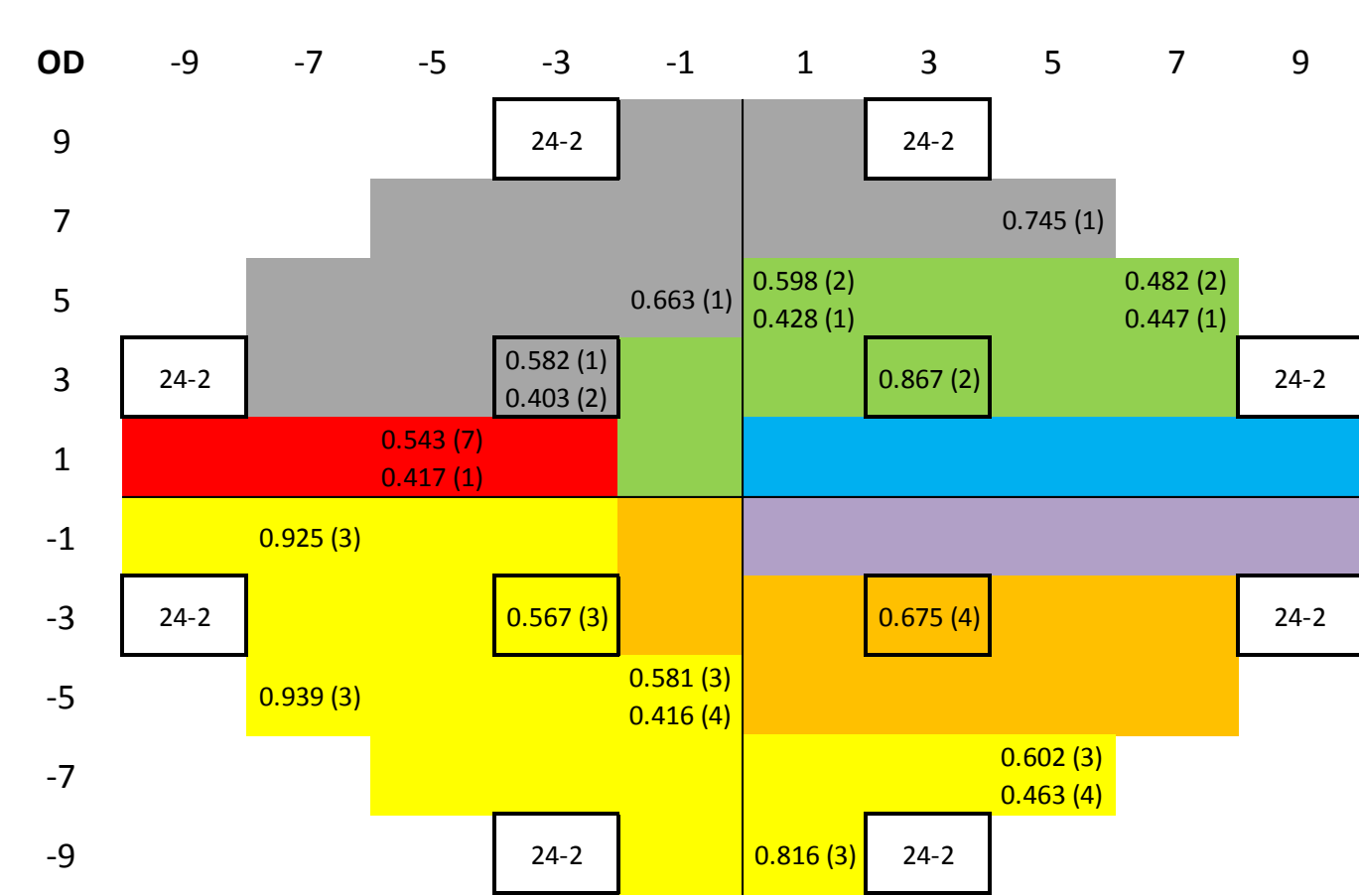
Superposition of the Panomap (ZEISS Cirrus SW V. 10.0) and the test locations within 10° in X- and Y-axis. Visual Field Orientation: The locations in this presentation are displaced corresponding to that in Hood DC, Raza AS, Method for comparing visual field defects to local RNFL and RGC damage seen on frequency domain OCT in patients with glaucoma. Biomed Opt Express. 2011 Apr 5;2(5):1097–1105- and are based upon a study by Drasdo, Millican, Katholi, and Curcio (2007). Turquoise dots represent the 10 new test locations. The dot size corresponds approximately with Goldmann stimulus size III (~0.5° diameter).

## References:

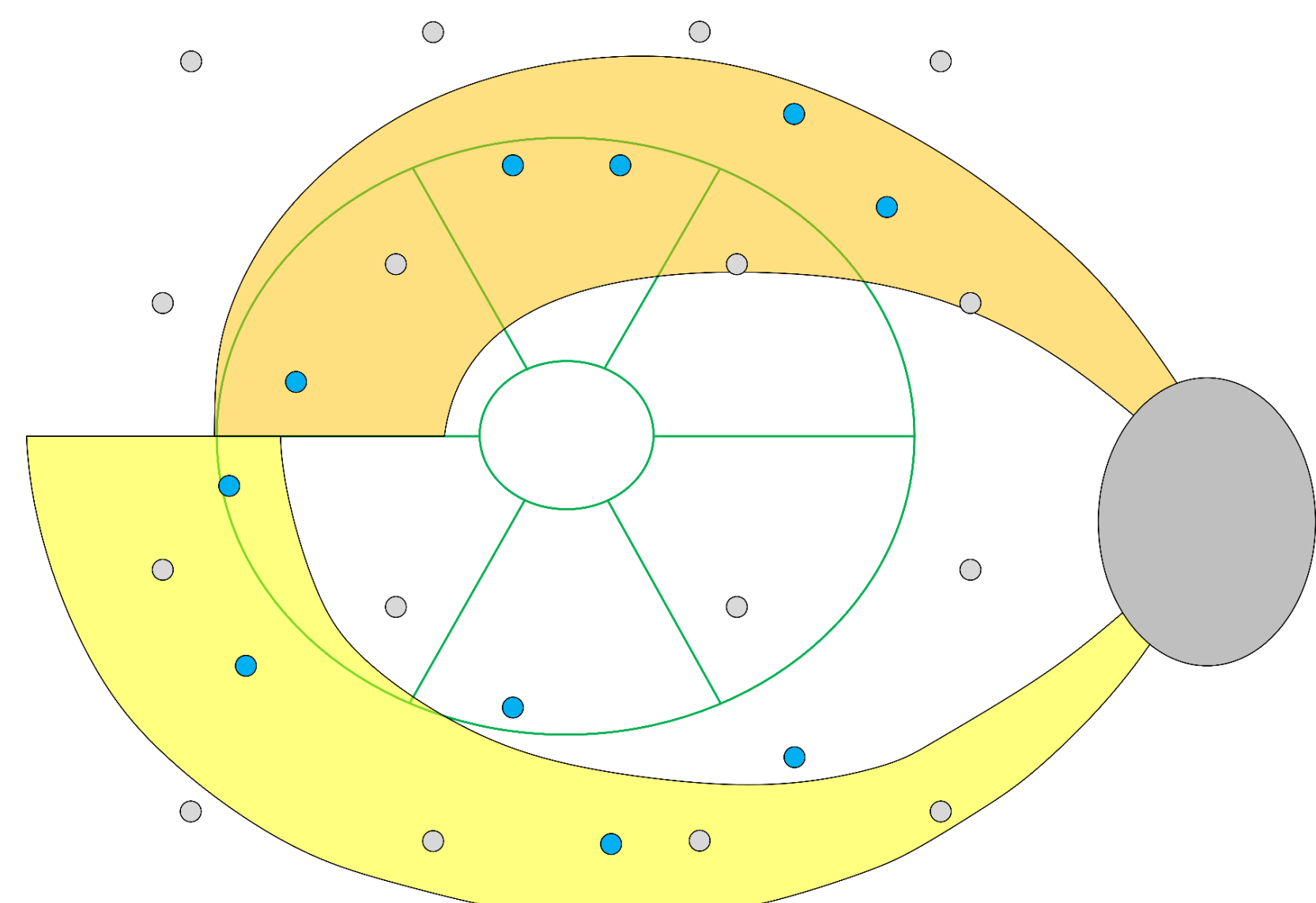
- Hood DC, Raza AS, de Moraes CGV, Johnson CA, Liebmann JM, Ritch R. The nature of macular damage in glaucoma as revealed by averaging optical coherence tomography data. *Trans Vis Sci Tech* 2012;1(1):3
- Schiefer U, Papageorgiou E, Sample PA, Pascual JP, Selig B, Krapp E, Paetzold J. Spatial pattern of glaucomatous visual field loss obtained with regionally condensed stimulus arrangements. *Invest Ophthalmol Vis Sci*. 2010 Nov;51(11):5685-9
- Hood DC, McKendrick AM, Swanson WH, Gardiner SK, Flanagan JG
- Ehrlich AC, Raza AS, Ritch R, Hood DC. Modifying the conventional visual field test pattern to improve the detection of early glaucomatous defects in the central 10°. *Tran Vis Sci Tech*. 2014;3(6):6,
- Chen S, McKendrick AM, Turpin A., Choosing two points to add to the 24-2 pattern to better describe macular visual field damage due to glaucoma., *Br J Ophthalmol*. 2015 Sep;99(9):1236-9. doi: 10.1136/bjophthalmol-2014-306431. Epub 2015 Mar 23.
- Traynis I, De Moraes CG, Raza AS, Liebmann JM, Ritch R, Hood DC. The Prevalence and Nature of Early Glaucomatous Defects in the Central 10° of the Visual Field. *JAMA ophthalmology*. 2014;132(3):291-297. doi:10.1001/jamaophthalmol.2013.7656
- Hood DC, Raza AS, de Moraes CG, Odel JG, Greenstein VC, Liebmann JM, Ritch R., Initial arcuate defects within the central 10 degrees in glaucoma., *Invest Ophthalmol Vis Sci*. 2011 Feb 16;52(2):940-6. doi: 10.1167/iovs.10-5803. Print 2011 Feb.
- Iwase A, Suzuki Y, Araie M; Tajimi Study Group., Characteristics of undiagnosed primary open-angle glaucoma: the Tajimi Study., *Ophthalmic Epidemiol*. 2014 Feb;21(1):39-44.
- de Moraes CG, Song C, Liebmann JM, Simonson JL, Furlanetto RL, Ritch R., Defining 10-2 visual field progression criteria: exploratory and confirmatory factor analysis using pointwise linear regression. *Ophthalmology*. 2014 Mar;121(3):741-9. doi: 10.1016/j.ophtha.2013.10.018. Epub 2013 Nov 28;.
- Hood DC, Raza AS, de Moraes CG, Liebmann JM, Ritch R., Glaucomatous damage of the macula, *Prog Retin Eye Res*. 2013 Jan;32:1-21. doi: 10.1016/j.preteyeres.2012.08.003. Epub 2012 Sep 17
- Kim H, Yang H, Lee TH, Lee KH. Diagnostic Value of Ganglion Cell-Inner Plexiform Layer Thickness in Glaucoma With Superior or Inferior Visual Hemifield Defects., *J Glaucoma*. 2016 Jun;25(6):472-6



These graphs show the originally suggested 9 additional paracentral test locations<sup>3</sup> and the result after reevaluation of test locations with a score of  $\leq 1$  applying the two rules described under "Methods".



These are the progression clusters as identified by de Moraes et al<sup>9</sup> and the loading factors calculated for the relevant test locations and their respective clusters. If the loading factor for a second cluster was  $\geq 0.4$ , two loading factors are shown. It appears likely – but has not been studied – that the neighboring test locations from the 24-2 could be included for cluster analysis.



This graph, derived from publications analyzing the vulnerability of the macula for glaucomatous damage<sup>10,11</sup> confirms, that the two most vulnerable zones are covered with 7 and 8 test locations respectively. Visual Field Orientation: Test locations displaced according to the length of the Henle fibers – for more details refer to the legend under the "Panomap" graphs.

Email: matthias.monhart@zeiss.com

Disclosures:  
MM(E): Carl Zeiss AG  
GL(E): Carl Zeiss Meditec, Inc.  
AI(P,R): Topcon, (R): Carl Zeiss Meditec, Santen, Alcon, Pfizer, Senju, Kowa, Ohtsuka  
JF(C): Carl Zeiss Meditec, Inc.

The authors like to thank all the members of the original expert group - Donald C. Hood, Stuart K. Gardiner, Allison M. McKendrick and William H. Swanson for their valuable contributions.